Spectra of Anti-Nucleons in the Vacuum of Finite Nuclei[*]

MAO Guang-Jun[1]

(Institute of High Energy Physics, Chinese Academy of Sciences, Beijing 100049, China)

(Institute of Theoretical Physics, Chinese Academy of Sciences, Beijing 100080, China)

(CCAST (World Lab.), Beijing 100080, China)

Abstract The quantum vacuum in a many-body system of finite nuclei has been investigated within the relativistic Hartree approach which describes the bound states of nucleons and anti-nucleons consistently. The contributions of the Dirac sea to the source terms of the meson-field equations are taken into account up to the one-nucleon loop and one-meson loop. The tensor couplings for the ω- and ρ-meson are included in the model. After adjusting the parameters of the model to the properties of spherical nuclei, a large effective nucleon mass $m^*/M_N \approx 0.78$ is obtained. The overall nucleon spectra of shell-model states are in agreement with the data. The computed anti-nucleon spectra in the vacuum differ about 20—30MeV with and without the tensor-coupling effects.

Key words spectra of anti-nucleons in vacuum, relativistic Hartree approach, tensor coupling

1 Introduction

One of the main characters distinguishing relativistic approaches from nonrelativistic approaches is that the former one has a vacuum. It is quite interesting to study the structure of quantum vacuum in a many-body system, e.g., in a finite nucleus where the Fermi sea is filled with the valence nucleons while the Dirac sea is full of the virtual nucleon—anti-nucleon pairs. A schematic picture taken from Refs. [1,2] is given in Fig.1. The shell-model states have been theoretically and experimentally well established[3] while no information for the bound states of anti-nucleons in the Dirac sea are available. This is the aim of our work. The observation of antinucleon bound states is a verification for the application of the relativistic quantum field theory to a many-body system[4]. It constitutes a basis for the widely used relativistic mean-field (RMF) theory under the no-sea approximation[2,4—8] and the relativistic Hartree approach (RHA)[9—13]. Since the bound states of nucleons are subject to the cancellation of two potentials $S + V$ (V is positive, S is negative) while the bound states of anti-nucleons, due to the G-parity, are sensitive to the sum of them S-V, consistent

studies of both the nucleon and the anti-nucleon bound states can determine the individual S and V. In addition, the exact knowledge of potential depth for anti-nucleons in the medium
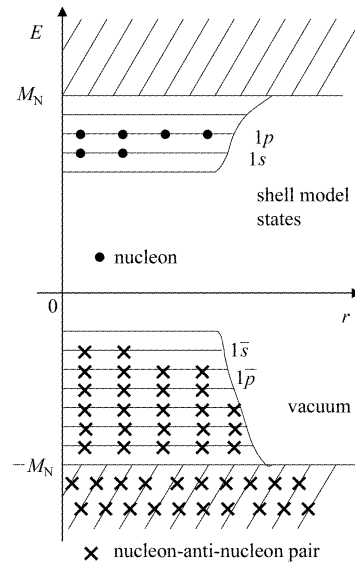

Fig.1. A schematic picture taken from Refs. [1,2] for the energy spectra in a finite nucleus. The shell-model states are filled with the valence nucleons while the vacuum is full of virtual nucleon-anti-nucleon pairs.

is a prerequisite for the study of anti-matter and anti-nuclei in relativistic heavy-ion collisions[14,15].

We have developed a relativistic Hartree approach which describes the bound states of nucleons and anti-nucleons in a unified framework. For the details of the model we refer to Refs. [16,17]. A brief description will be given in Sec. 2. Numerical results and discussions are presented in Sec. 3.

2　Relativistic Hartree approach

The Lagrangian density of nucleons interacting through the exchange of mesons can be expressed as[4]

$$\mathcal{L} = \overline{\psi}[i\gamma_\mu \partial^\mu - M_N]\psi + \frac{1}{2}\partial_\mu\sigma\partial^\mu\sigma - U(\sigma) - \frac{1}{4}\omega_{\mu\nu}\omega^{\mu\nu} +$$
$$\frac{1}{2}m_\omega^2\omega_\mu\omega^\mu - \frac{1}{4}\boldsymbol{R}_{\mu\nu}\cdot\boldsymbol{R}^{\mu\nu} + \frac{1}{2}m_\rho^2\boldsymbol{R}_\mu\cdot\boldsymbol{R}^\mu - \frac{1}{4}A_{\mu\nu}A^{\mu\nu} +$$
$$g_\sigma\overline{\psi}\psi\sigma - g_\omega\overline{\psi}\gamma_\mu\psi\omega^\mu - \frac{f_\omega}{4M_N}\overline{\psi}\sigma^{\mu\nu}\psi\omega_{\mu\nu} - \frac{1}{2}g_\rho\overline{\psi}\gamma_\mu\boldsymbol{\tau}\cdot\psi\boldsymbol{R}^\mu -$$
$$\frac{f_\rho}{8M_N}\overline{\psi}\sigma^{\mu\nu}\boldsymbol{\tau}\cdot\psi\boldsymbol{R}_{\mu\nu} - \frac{1}{2}e\overline{\psi}(1+\tau_0)\gamma_\mu\psi A^\mu, \quad (1)$$

where $U(\sigma)$ is the self-interaction part of the scalar field[18]

$$U(\sigma) = \frac{1}{2}m_\sigma^2\sigma^2 + \frac{1}{3!}b\sigma^3 + \frac{1}{4!}c\sigma^4. \quad (2)$$

In the above f_ω and f_ρ are the tensor-coupling strengths of vector mesons; other symbols have their usual meaning.

In finite nuclei the Dirac equation is written as

$$i\frac{\partial}{\partial t}\psi(\boldsymbol{x},t) = \left[-i\boldsymbol{\alpha}\cdot\boldsymbol{\nabla} + \beta(M_N - g_\sigma\sigma(\boldsymbol{x})) + \right.$$
$$g_\omega\omega_0(\boldsymbol{x}) - \frac{f_\omega}{2M_N}i\boldsymbol{\gamma}\cdot(\boldsymbol{\nabla}\omega_0(\boldsymbol{x})) +$$
$$\frac{1}{2}g_\rho\tau_0 R_{0,0}(\boldsymbol{x}) - \frac{f_\rho}{4M_N}i\tau_0\boldsymbol{\gamma}\cdot(\boldsymbol{\nabla}R_{0,0}(\boldsymbol{x})) +$$
$$\left. \frac{1}{2}e(1+\tau_0)A_0(\boldsymbol{x}) \right]\psi(\boldsymbol{x},t). \quad (3)$$

The field operator can be expanded according to nucleons and anti-nucleons and reads as

$$\psi(\boldsymbol{x},t) = \sum_\alpha [b_\alpha\psi_\alpha(\boldsymbol{x})e^{-iE_\alpha t} + d_\alpha^+\psi_\alpha^a(\boldsymbol{x})e^{i\overline{E}_\alpha t}]. \quad (4)$$

Here the label α denotes the full set of single-particle quantum numbers. The wave functions of nucleons and anti-nucleons can be specified as[19,16]

$$\psi_\alpha(\boldsymbol{x}) = \begin{pmatrix} i\dfrac{G_\alpha(r)}{r}\Omega_{jlm}\left(\dfrac{\boldsymbol{r}}{r}\right) \\ \dfrac{F_\alpha(r)}{r}\dfrac{\boldsymbol{\sigma}\cdot\boldsymbol{r}}{r}\Omega_{jlm}\left(\dfrac{\boldsymbol{r}}{r}\right) \end{pmatrix}, \quad (5)$$

$$\psi_\alpha^a(\boldsymbol{x}) = \begin{pmatrix} -\dfrac{\overline{F}_\alpha(r)}{r}\dfrac{\boldsymbol{\sigma}\cdot\boldsymbol{r}}{r}\Omega_{jlm}\left(\dfrac{\boldsymbol{r}}{r}\right) \\ i\dfrac{\overline{G}_\alpha(r)}{r}\Omega_{jlm}\left(\dfrac{\boldsymbol{r}}{r}\right) \end{pmatrix}. \quad (6)$$

here Ω_{jlm} are the spherical spinors.

Inserting Eq. (4) into Eq. (3) and making some straightforward algebra we arrive at the Schrödinger-equivalent equations for the upper component of the nucleon's wave function

$$E_\alpha G_\alpha(r) = \left[-\frac{d}{dr} + W(r) \right]M_{eff}^{-1}\left[\frac{d}{dr} + W(r) \right]G_\alpha(r) + U_{eff}G_\alpha(r), \quad (7)$$

and the lower component of the anti-nucleon's wave function

$$\overline{E}_\alpha\overline{G}_\alpha(r) = \left[-\frac{d}{dr} + \overline{W}(r) \right]\overline{M}_{eff}^{-1}\left[\frac{d}{dr} + \overline{W}(r) \right]\overline{G}_\alpha(r) + \overline{U}_{eff}\overline{G}_\alpha(r). \quad (8)$$

Other components can be obtained through the following relations

$$F_\alpha(r) = M_{eff}^{-1}\left[\frac{d}{dr} + W(r) \right]G_\alpha(r), \quad (9)$$

$$\overline{F}_\alpha(r) = \overline{M}_{eff}^{-1}\left[\frac{d}{dr} + \overline{W}(r) \right]\overline{G}_\alpha(r). \quad (10)$$

The Schrödinger-equivalent effective mass and potentials are defined as follows: for the nucleon

$$M_{eff} = E_\alpha + M_N - g_\sigma\sigma(r) - g_\omega\omega_0(r) - \frac{1}{2}g_\rho\tau_{0\alpha}R_{0,0}(r) - \frac{1}{2}e(1+\tau_{0\alpha})A_0(r), \quad (11)$$

$$U_{eff} = M_N - g_\sigma\sigma(r) + g_\omega\omega_0(r) + \frac{1}{2}g_\rho\tau_{0\alpha}R_{0,0}(r) + \frac{1}{2}e(1+\tau_{0\alpha})A_0(r), \quad (12)$$

$$W(r) = \frac{\kappa_\alpha}{r} - \frac{f_\omega}{2M_N}(\partial_r\omega_0(r)) - \frac{f_\rho}{4M_N}\tau_{0\alpha}(\partial_r R_{0,0}(r)), \quad (13)$$

for the anti-nucleon

$$\overline{M}_{eff} = \overline{E}_\alpha + M_N - g_\sigma\sigma(r) + g_\omega\omega_0(r) - \frac{1}{2}g_\rho\tau_{0\alpha}R_{0,0}(r) + \frac{1}{2}e(1+\tau_{0\alpha})A_0(r), \quad (14)$$

$$\overline{U}_{eff} = M_N - g_\sigma\sigma(r) - g_\omega\omega_0(r) + \frac{1}{2}g_\rho\tau_{0\alpha}R_{0,0}(r) - \frac{1}{2}e(1+\tau_{0\alpha})A_0(r), \quad (15)$$

$$\overline{W}(r) = \frac{\kappa_\alpha}{r} + \frac{f_\omega}{2M_N}(\partial_r\omega_0(r)) - \frac{f_\rho}{4M_N}\tau_{0\alpha}(\partial_r R_{0,0}(r)). \quad (16)$$

One can see that the difference between the equations of nucleons and anti-nucleons relies only on the definition of the effective masses and potentials, that is, the vector fields change their signs. The G-parity comes out automatically. The main ingredients of the equations are meson fields which can be obtained through solving the Laplace equations of mesons in spherical nuclei. The source terms of the meson-

field equations are various densities containing the contributions both from the valence nucleons and the Dirac sea. They are evaluated by means of the derivative expansion technique[20]. In numerical calculations the Laplace equations and the equations of nucleons and anti-nucleons are solved in an iterative procedure self-consistently to determine the potentials and wave functions. The energy spectra of the nucleon and the anti-nucleon are computed by means of the following equations

$$E_\alpha = \int_0^\infty dr \Big\{ G_\alpha(r) \Big[-\frac{d}{dr} + W(r) \Big] F_\alpha(r) +$$

$$F_\alpha(r) \Big[\frac{d}{dr} + W(r) \Big] G_\alpha(r) + G_\alpha(r) U_{eff} G_\alpha(r) -$$

$$F_\alpha(r) [M_{eff} - E_\alpha] F_\alpha(r) \Big\}, \tag{17}$$

$$\bar{E}_\alpha = \int_0^\infty dr \Big\{ \bar{G}_\alpha(r) \Big[-\frac{d}{dr} + \bar{W}(r) \Big] \bar{F}_\alpha(r) +$$

$$\bar{F}_\alpha(r) \Big[\frac{d}{dr} + \bar{W}(r) \Big] \bar{G}_\alpha(r) + \bar{G}_\alpha(r) \bar{U}_{eff} \bar{G}_\alpha(r) -$$

$$\bar{F}_\alpha(r) [\bar{M}_{eff} - \bar{E}_\alpha] \bar{F}_\alpha(r) \Big\}. \tag{18}$$

3 Numerical results and discussions

The parameters of the model are fixed in a least-square fit to the properties of eight spherical nuclei. They are presented in Table 1 and denoted as the RHAT set and the RHA1 set for the two cases of with and without the tensor-

Table 1. **Parameters of the RHA models as well as the corresponding saturation properties.** M_N and m_ρ are fixed during the fit.

	RHA1	RHAT
M_N/MeV	938.000	938.000
m_σ/MeV	458.000	450.000
m_ω/MeV	816.508	814.592
m_ρ/MeV	763.000	763.000
g_σ	7.1031	7.0899
g_ω	8.8496	9.2215
g_ρ	10.2070	11.0023
b/fm^{-1}	24.0870	18.9782
c	-15.9936	-27.6894
(f_ω/M_N)/fm	0.0	2.0618
(f_ρ/M_N)/fm	0.0	45.3318
ρ_0/fm^{-3}	0.1524	0.1493
(E/A)/MeV	-16.98	-16.76
m^*/M_N	0.788	0.779
K/MeV	294	311
a_4/MeV	40.4	44.0

coupling terms. The major result is that a large effective nucleon mass $m^*/M_N \approx 0.78$ is obtained. The contributions of the vacuum to the scalar density and baryon density are depicted in Fig. 2. The computations are performed with the RHAT set of parameters for ^{40}Ca. Noticeable influence from the Dirac sea can be found for the scalar density while the effect on the baryon density is relatively small.
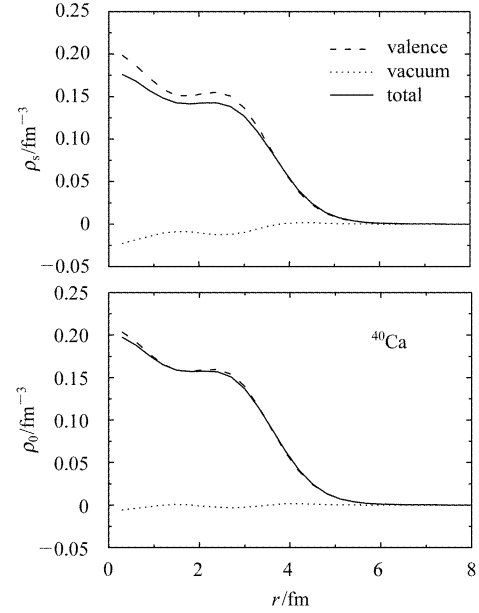

Fig.2. The scalar density and baryon density in ^{40}Ca. Dashed lines denote the contributions of valence nucleons, dotted lines represent the Dirac-sea effects and solid lines give the total results.

In Table 2 and 3 we present the single-particle energies of protons (neutrons) and anti-protons (anti-neutrons) in three spherical nuclei of ^{16}O, ^{40}Ca and ^{208}Pb. The binding energies per nucleon and the rms charge radii are given too. The experimental data are taken from Ref. [21]. It can be found that the relativistic Hartree approach taking into account the vacuum effects can reproduce the observed binding energies, rms charge radii and particle spectra quite well. Because of the large effective nucleon mass, the spin-orbit splitting on the 1p levels is rather small in the RHA1 model. The situation has been ameliorated conspicuously in the RHAT model incorporating the tensor couplings for the ω-and ρ-meson, while a large m^* stays unchanged. On the other hand, the anti-particle energies computed with the RHAT set of parameters are 20—30MeV larger than that reckoned with the RHA1 set.

Table 2. The single-particle energies of both protons and anti-protons as well as the binding energies per nucleon and the *rms* charge radii in ^{16}O, ^{40}Ca and ^{208}Pb.

	RHA1	RHAT	Expt.
^{16}O			
(E/A)/MeV	8.00	7.94	7.98
r_{ch}/fm	2.66	2.64	2.74
PROTONS			
$1s_{1/2}$/MeV	30.68	31.63	40 ± 8
$1p_{3/2}$/MeV	15.23	16.18	18.4
$1p_{1/2}$/MeV	13.24	12.22	12.1
ANTI-PRO			
$1\bar{s}_{1/2}$/MeV	299.42	328.55	
$1\bar{p}_{3/2}$/MeV	258.40	283.44	
$1\bar{p}_{1/2}$/MeV	258.93	285.87	
^{40}Ca			
(E/A)/MeV	8.73	8.62	8.55
r_{ch}/fm	3.42	3.41	3.45
PROTONS			
$1s_{1/2}$/MeV	36.58	37.01	50 ± 11
$1p_{3/2}$/MeV	25.32	25.95	
$1p_{1/2}$/MeV	24.03	23.63	34 ± 6
ANTI-PRO			
$1\bar{s}_{1/2}$/MeV	339.83	367.90	
$1\bar{p}_{3/2}$/MeV	309.24	332.10	
$1\bar{p}_{1/2}$/MeV	309.52	333.37	
^{208}Pb			
(E/A)/MeV	7.93	7.88	7.87
r_{ch}/fm	5.49	5.46	5.50
PROTONS			
$1s_{1/2}$/MeV	40.80	41.74	
$1p_{3/2}$/MeV	36.45	37.38	
$1p_{1/2}$/MeV	36.21	37.18	
ANTI-PRO			
$1\bar{s}_{1/2}$/MeV	354.18	377.37	
$1\bar{p}_{3/2}$/MeV	344.48	366.95	
$1\bar{p}_{1/2}$/MeV	344.52	367.24	

Table 3. The single-particle energies of both neutrons and anti-neutrons.

	RHA1	RHAT	Expt.
^{16}O			
NEUTRONS			
$1s_{1/2}$/MeV	34.71	35.78	45.7
$1p_{3/2}$/MeV	19.04	20.18	21.8
$1p_{1/2}$/MeV	17.05	15.75	15.7
ANTI-NEU			
$1\bar{s}_{1/2}$/MeV	293.23	322.47	
$1\bar{p}_{3/2}$/MeV	252.48	277.94	
$1\bar{p}_{1/2}$/MeV	252.97	279.22	
^{40}Ca			
NEUTRONS			
$1s_{1/2}$/MeV	44.48	44.98	
$1p_{3/2}$/MeV	32.98	33.83	
$1p_{1/2}$/MeV	31.71	30.99	
ANTI-NEU			
$1\bar{s}_{1/2}$/MeV	327.96	355.70	
$1\bar{p}_{3/2}$/MeV	298.04	321.07	
$1\bar{p}_{1/2}$/MeV	298.26	322.15	
^{208}Pb			
NEUTRONS			
$1s_{1/2}$/MeV	47.40	46.70	
$1p_{3/2}$/MeV	42.66	42.31	
$1p_{1/2}$/MeV	42.45	41.64	
ANTI-NEU			
$1\bar{s}_{1/2}$/MeV	313.18	334.39	
$1\bar{p}_{3/2}$/MeV	304.61	325.41	
$1\bar{p}_{1/2}$/MeV	304.61	325.28	

References

1　Auerbach N et al. Phys. Lett.,1986,**B182**:221

2　Reinhard P G et al. Z. Phys.,1986,**A323**:13

3　Bohr A, Mottelson B R. Nuclear Structure (Benjamin W A. New York, 1969)

4　Serot B D, Walecka J D, Adv. Nucl. Phys.,1986,**16**:1

5　Gambhir Y K, Ring P, Thimet A. Ann. Phys.,1990,**198**:132

6　REN Z Z et al. Phys. Lett.,1996, **B380**:241

7　MENG J et al. Phys. Rev.,1998,**C58**:R628

8　Sugahara Y, Toki H. Nucl. Phys.,1994,**A579**:557

9　Horowitz C J, Serot B D. Phys. Lett.,1984,**B140**:181

10　Perry R J. Phys. Lett.,1986,**B182**:269; Nucl. Phys.,1987,**A467**:717

11　Wasson D A. Phys. Lett.,1988,**B210**:41

12　Fox W R. Nucl. Phys.,1989, **A495**:463

13　Furnstahl R J, Price C E. Phys. Rev.,1989,**C40**:1398; Phys. Rev., 1990, **C41**:1792

14　Bearden I G et al. Phys. Rev. Lett.,2000, **85**:2681

15　Armstrong T A(E864 Collab.). Phys. Rev. Lett.,2000, **85**:2685

16　Mao G, Stöcker H, Greiner W. Int. J. Mod. Phys.,1999,**E8**:389; AIP Conf. Proc.,2001,**597**:112

17　MAO G J. Phys. Rev.,2003, **C67**:044318; HEP&NP,2003,**27**:692 (in Chinese)
(茅广军. 高能物理与核物理,2003,27:692)

18　Boguta J, Bodmer A R. Nucl. Phys.,1997,**A292**:413

19　Bjorken J D, Drell S D. Relativistic Quantum Mechanics (McGraw-Hill, New York, 1964)

20　Aitchison I J R, Fraser C M. Phys. Lett.,1984,**B146**: 63; Cheyette O. Phys. Rev. Lett.,1985, **55**:2394; Fraser C M. Z. Phys.,1985, **C28**:101; Chan L H. Phys. Rev. Lett.,1985, **54**:1222

21　Mattauch J H E, Thiele W, Wapstra A H. Nucl. Phys.,1965,**67**:1; Vautherin D, Brink D M. Phys. Rev.,1972,**C5**:626; de Vries H, de Jager C W, de Vries C. At. Data Nucl. Data Tables,1987, **36**:495

有限核真空中的反核子能谱 *

茅广军[1)]

(中国科学院高能物理研究所　北京　100049)

(中国科学院理论物理研究所　北京　100080)

(中国高等科学技术中心世界实验室　北京　100080)

摘要　通过建立能够自洽地描述核子和反核子束缚态的相对论 Hartree 模型来研究有限核中的量子真空,其中狄拉克海对介子场方程的贡献由单圈图考虑,模型中还引入了 ω 介子和 ρ 介子的张量耦合项. 在拟合球形核的性质后得到模型的参数,给出核子有效质量为 $m^*/M_N \approx 0.78$;计算得到的核子壳模型能级与实验值相一致,在考虑张量耦合项的效应后真空反核子位阱深度增大了 20—30 MeV.

关键词　真空反核子能谱　相对论 Hartree 模型　张量耦合